Applied Catalysis B: Environmental 250 (2019) 292–300

Contents lists available at ScienceDirect

Applied Catalysis B: Environmental

journal homepage: www.elsevier.com/locate/apcatb

Engineering a cobalt clathrochelate/glassy carbon interface for the hydrogen evolution reaction

Joumada Al Cheikh, Angel Villagra, Alireza Ranjbari, Alexandre Pradon, Manuel Antuch, Diana Dragoe, Pierre Millet, Loïc Assaud*

Institut de Chimie Moléculaire et des Matériaux d'Orsay (ICMMO) – ERIEE, Université Paris-Sud, Université Paris-Saclay, CNRS, Rue du Doyen Georges Poitou, 91400, Orsay, France

ARTICLE INFO

Keywords:
Hydrogen
Electrocatalysis
Cobalt clathrochelate
Electrografting
HER

ABSTRACT

The purpose of this work was to investigate the electrocatalytic activity of a molecular clathrochelate, containing cobalt as active centre, for the hydrogen evolution reaction (HER) in aqueous acidic media. The electrocatalytic activity of this cobalt complex has been measured using a glassy carbon working electrode, with the complex either dissolved in the electrolyte (homogeneous phase) or electro-grafted at the surface (heterogeneous phase). The complex was electrografted via diazonium derivatives reduction, in an attempt to form a surface monolayer of cobalt clathrochelate, covalently bonded to the glassy carbon substrate. The chemical composition and morphology of the modified electrode have been characterized by electron microscopy, atomic force microscopy and X-ray photoelectron spectroscopy. The HER kinetics on the two electrodes has been analyzed by cyclic voltammetry and electrochemical impedance spectroscopy in two different media: in acetonitrile (by adding increasing amounts of equivalent protons) and in 0.1 M H_2SO_4 aqueous solution. Tafel slopes and exchange current density values have been determined on both electrodes, in both media, and compared. It was found that the onset of the HER requires a significantly lower overpotential ($\approx$ 800 mV less) when the complex is electrografted at the surface of the working electrode. The hydrogen production rate, determined by gas chromatography, is reported.

1. Introduction

The R&D on new processes for the large scale production of low-cost electrolytic dihydrogen from carbon-free feedstocks such as water has been significantly increased over the last years. Among several other technologies, water electrolysis is considered as a key process for the chemical storage of intermittent and renewable energy sources. There are currently three main water electrolysis technologies available on the market. They differ by their operating temperature and pressure conditions, and by the pH of the electrolyte [1]. Among these, the polymer electrolyte membrane (PEM) technology is considered as the most appropriate one for grid services [2]. The pH of the polymer electrolyte used in these cells is equivalent to that of a 1 M sulfuric acid solution. To avoid corrosion and catalyst dissolution issues, scarce and expensive platinum group metals (PGM) electrocatalysts are used, usually platinum nanoparticles supported on carbon for the hydrogen evolution reaction (HER) at the cathode, and unsupported iridium dioxide particles at the anode for the oxygen evolution reaction (OER) [3]. The current research effort on alternative HER electrocatalysts is made to replace platinum by transition metals, mainly Fe, Ni, Co [4–7]. Because these metals are not chemically stable in acidic aqueous media at open circuit conditions, an alternative solution is to use molecular complexes [8]. Alternative catalysts based on molecular chemistry have been reported as cathodic or anodic material for water electrolysis [2]. Indeed, numerous complexes containing a cobalt metallic electro-active center, e.g. systems containing macrocyclic and polypyridine ligands, have been reported as electrocatalysts for dihydrogen production by electrochemical reduction of protons from different proton sources in the last twenty years [9–16]. These molecular catalysts can be used either dissolved in the electrolyte (homogeneous phase) or functionalized at the surface of a solid but electrochemically inert supporting electrode (e.g. carbonaceous species) for applications. Various procedures such as drop-casting, dip coating or electro-grafting have been reported in the literature for surface functionalization of molecular active centers. The latter technique is making reference to the electrochemical reaction that allows organic layers to be covalently bonded to a solid conductive substrate such as glassy carbon (GC) or gold [17–19]. This definition can be extended to reactions involving an electron

* Corresponding author.
E-mail address: loic.assaud@u-psud.fr (L. Assaud).

https://doi.org/10.1016/j.apcatb.2019.03.036
Received 3 August 2018; Received in revised form 5 March 2019; Accepted 13 March 2019
Available online 16 March 2019

transfer between the substrate and the reagent, but also to examples where a reducing or oxidizing reagent is added to produce the reactive species. These methods are interesting to produce electrochemical interfaces because strong covalent chemical bonds can form between the surface and the electroactive molecular layer. Electrografting has been applied so far to a variety of substrates including carbon, metals and metal-oxides, but also dielectrics such as polymers. Since the 1980s several methods have been developed, either by reduction or oxidation, and some of them have been even used at industrial scales [20].

The main objective of our study was to compare the electroactivity and chemical stability of a known HER molecular electrocatalyst, when it is dissolved in solution, and when it is electrografted at the surface of a GC working electrode. Many molecular cobalt complexes have recently been investigated and identified as potential electrocatalysts both for the hydrogen evolving reaction (HER) and oxygen evolving reaction (OER) [21–24]. Among them, cobalt tri glyoxime complexes such as the dimethyl substituted compounds, have been particularly studied as catalysts for the HER in aprotic solvents and different HER mechanistic pathways have been proposed [25]. In a recent investigation, the high HER electroactivity of a fluoroboryl-capped tris-(glyoximato) diphenyl cobalt clathrochelate complex in solution in acetonitrile has been reported in the presence of acid [26,27]. We selected this cobalt clathrochelate as the best candidate for our purpose because of its appropriate HER electroactivity and appropriate chemical structure required for surface functionalization by electrografting via the peripheral carboxylic groups. Also, the complex is soluble in acetonitrile and almost insoluble in water.

2. Experimental section

All chemicals were obtained either from Sigma Aldrich or Carl Roth and used as received. Water was purified in a Millipore system. Cobalt complexes were synthesized using a procedure reported elsewhere [27]. Scanning electron micrographs were acquired with a Zeiss Supra 55 VP variable pressure scanning electron microscope with field emission gun (SEM-FEG), equipped with energy dissipative X-ray spectroscopy (EDS) for chemical microanalysis. Atomic force microscopy was performed on an ICON Brüker microscope in peakforce tapping mode, using a scan asyst probe. X-ray photoelectron spectroscopy was performed using a Thermo Fisher Scientific spectrometer equipped with a monochromatic Al K_α source (1486.7 eV) using a spot of 400 µm in size and a hemispherical analyzer, at a take-off angle of 0°. The acquisition and fitting of spectra were performed with Thermo Avantage software, whereby a Shirley background was used. The binding energy scale was calibrated with respect to the C1s peak located at 284.8 eV. Electrochemical characterizations were performed after deaeration of the electrolyte using an argon flow. Cyclic voltammograms and electrochemical impedance spectroscopy were recorded using a Voltalab potentiostat (from Radiometer) in a three-electrode configuration setup using a Pt plate and a saturated calomel electrode ($E°_{SCE}$ = 242 mV vs. NHE) as counter electrode and reference, respectively. The clathrochelate complexes were dissolved in acetonitrile to a final concentration of 0.2 mM when characterized in the homogenous phase and in dimethylfluoramide when characterized in the heterogeneous phase, using 0.1 M tetrabutylammonium perchlorate as supporting electrolyte. Note that the concentration of the clathrochelate in solution in acetonitrile has been empirically optimized (a value of 0.2 mM has been determined) in order to obtain as thin as possible surface deposits. The results reported in this paper were obtained with this optimized concentration only. Glassy carbon disk electrodes (GC, 0.07 cm^2) were used as working electrodes. GC electrodes were carefully polished before each measurement using successively 6 µm, 3 µm, and 1 µm diamond paste. Electrolysis for the hydrogen evolution reaction was performed by adding controlled amounts of an aqueous solution of formic acid to the electrochemical cell in both homogenous (catalyst in solution) and heterogeneous (catalyst grafted to the solid electrode) phases. Potentials in non-aqueous media were referred to the formal equilibrium potential of ferrocene that was measured against a SCE in the same conditions employed for all other electrochemical experiments ($E^{\circ'}$ = 420 mV vs. SCE, taking into account the liquid junction potential). All electrode potentials are thus referred to the redox potential of ferrocene for experiments carried out in organic solutions and referred to SCE for experiments carried out in water. Electrochemical impedance spectroscopy was performed over the 50 kHz–20 mHz frequency range, at a potential of –1.5 V vs. SCE. Gas chromatography measurements were carried out using a Perkin Elmer Clarus 580 gas chromatograph equipped with both a thermal conductivity detector (TCD) and flame ionization detector (FID). The retention time was measured in order to quantitatively determine the dihydrogen production. In this case, a carbon plate was used as a counter electrode during the electrolysis. UV–vis spectra were recorded in transmission mode using a Cary 60 spectrometer from Agilent Technologies.

3. Results and discussion

3.1. Electro-grafting of diazonium salts —NO_2 derivatives

Fig. 1 provides a schematic overview of the electrografting process.

The same methodology can be used for grafting on a variety of substrates such as carbon, metals, semiconductors, oxides and polymers [17]. The synthesis can be performed in aprotic medium (acetonitrile), in the presence of *tert*-butyl nitrite. In an even simpler manner, it is also possible to prepare the diazonium salt *in situ* in the electrochemical cell by mixing, in an aqueous acidic solution, the aromatic amine and sodium nitrite and directly performing the electrolysis or the spontaneous reaction [29]. Whatever the method used for the production of 4-nitrobenzenediazonium, it is necessary to start from an aromatic amine, a large number of these compounds being commercially available. In the present study, the grafting of the diazonium derivative (4-nitrobenzenediazonium) was prepared using a classical multi-step synthesis procedure [28]: an aromatic amine was first mixed with sodium nitrite in an ice-cold aqueous acidic solution; then the mixture was filtered, and the solid precipitate was washed with the acidic solution. The diazonium salt was then electrochemically reduced by cyclic voltammetry. Fig. 2a shows the cyclic voltammograms (CVs) measured during the first step of the electrografting process. The first scan exhibits a well-defined and broad irreversible cathodic wave at –0.6 V vs. SCE obtained from 4-nitrobenzenediazonium in aqueous solution. This wave is not present on the subsequent second, third, and fourth cycles.

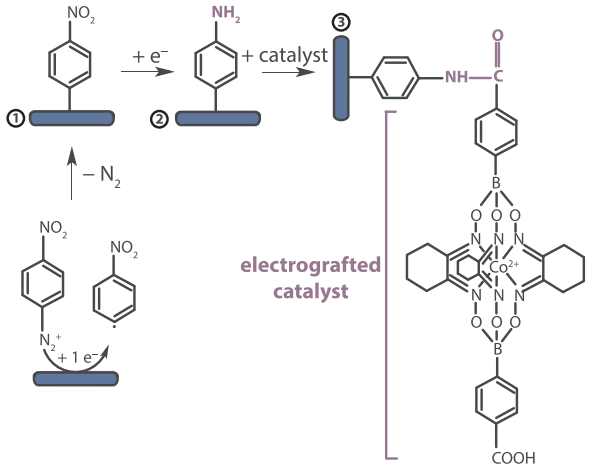

Fig. 1. Schematic overview of the catalytic modified electrode elaboration and functionalization. It consists of diazonium derivative electrogratfing (steps 1, 2) followed by the Co clathrochelate-based catalyst chemical grafting to the solid electrode surface (step 3).

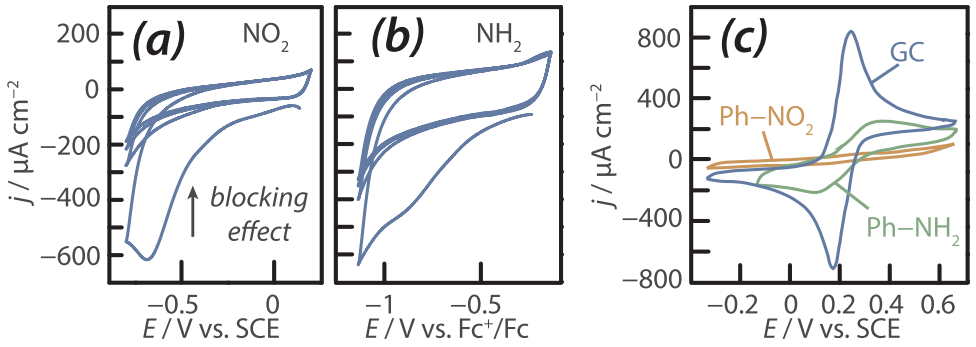

Fig. 2. Cyclic voltammograms recorded on a glassy carbon electrode modified by (a) grafting of 4-nitrobenzenediazonium (C = 2 mM) in 0.5 M HCl followed by (b) electroreduction of the diazonium derivative to amine (NH_2) in 4:1 H_2O : CH_3OH + 0.1 M Na_2SO_4. (c) Cyclic voltammogram of a modified glassy carbon electrode before and after grafting of a Ph-NH_2 group in the presence of the ferricyanide / ferrocyanide (5 mM) couple in aqueous medium. Scanning rate: ν = 50 mV s^{-1}.

Such behavior is very typical of the electrochemistry of these compounds. The disappearance of the electrochemical wave is related to the formation of an organic surface layer which, once formed, is blocking the access of the electroactive diazonium species to the electrode surface until a self-limited coverage of the whole surface electrode is obtained. On carbon, it has also been proposed that the different peaks might be related to the different crystalline structures available on the surface (e.g. graphitic planes and edges) [30]. Indeed, the electrografting functionalization was performed on a glassy carbon electrode. Such materials/surfaces exhibit a poor order, and are more complex than graphene surfaces. Moreover, the surface contains a multitude of hydrogen and oxygen functional groups, as well as radical sites to which the diazonium species could tend to bind [31].

The electrochemical reaction involved in the CVs of Fig. 2a is a one electron transfer process from the GC working electrode to the diazonium cation, in order to form an aryl radical (see Fig. 1). The radical was then reduced to form an anion at more negative potentials (–0.6 V vs. SCE). By using electron spin resonance (ESR) analysis performed at very low temperature, it has been shown elsewhere [32,33] that diazenyl radicals (Ar–N = $N^{\bullet}$) could form as intermediate species during the process. Such finding suggests that the electrochemical activation barrier is not high enough to put into evidence the formation of the diazenyl radical species, and that such species can only be detected by using auxiliary techniques such as ESR [32,34]. Therefore, the mechanism taking place probably involves additional radicals, not identifiable by cyclic voltammetry. The reduction potential of the phenyl radical has been determined by experiments at very low concentrations, for which grafting becomes inefficient. Under such operating conditions, a second wave of small magnitude is observed at the potential of –0.3 V. This wave is attributed to the reduction of the residual radicals that did not react through other reactions during the time required to drive the scanning potential to the reduction potential of the species [35]. These CVs also revealed a concerted electron transfer and cleavage of the dinitrogen molecule.

3.2. Electroreduction of $-NO_2$ to $-NH_2$

Once the nitrophenyl (Ph–NO_2) species are electrografted to the surface of the GC working electrode, it becomes possible to transform the –NO_2 group into a primary amine (–NH_2) group. This was achieved electrochemically, again by cyclic voltammetry, in an aqueous solution, by applying a scanning linear potential from 0.0 V down to –1.1 V vs. SCE at a potential scan rate of 50 mV.s^{-1}. Fig. 2b shows the CVs recorded during this second step. An electrochemical cathodic wave was observed at –0.8 V. This wave is attributed to the irreversible reduction of –NO_2 to –NH_2 at the working potential of –0.8 V. The intensity of the cathodic current was significantly reduced during the subsequent scans. These features are due to the transformation of all nitro groups into amine groups, inducing a self-limiting blocking organic layer that inhibits electron transfer. Indeed, these results suggest a compact layer of aminophenyl groups, strongly attached to the glassy carbon surface, which tends to passivate the electrode and leads to limit the electron transfer. This is once again very typical of the electrochemical behavior of these compounds.

3.3. Chemical grafting of the Co clathrochelate electrocatalyst

The cobalt clathrochelate complex was then chemically grafted to the diazonium derivative covered GC working electrode by electrografting. This was done simply by adding the cobalt clathrochelate and 1 M equivalent of dicyclohexylcarbodiimide to the reactional medium in order to catalyse the amide formation. This lead to the formation of covalent bonds between the carboxilic acid terminations of the clathrochelate and the amine functions of the carbon electrode.

3.4. Barrier effect of the modified electrochemical interface

The resulting modified GC working electrode has a blocking behavior: charge transfer is mostly inhibited. This was put into evidence by cyclic voltammetry, in the presence of ferri/ferrocyanide as an electroactive redox mediator. Fig. 2c shows three CVs. The first one (blue line) was recorded on the bare GC working electrode, the second one (orange line) and the third one (green line) respectively before and after the electrografting of the in situ generated 4-aminophenyl diazonium cations [36]. The electrochemical response of the bare GC electrode in presence of the ferri/ferrocyanide redox couple was then significantly affected by the grafted layers. The CVs obtained when the GC working electrode is covered by aminophenyl groups (green line) instead of nitrophenyl groups (orange line) show a larger decay of the electrochemical response of the $[Fe(CN)_6]^{3-/4-}$ redox couple. These methodological tests have been performed to confirm that the glassy carbon working electrode surface was adequately modified and homogeneously covered.

Fig. 3 shows scanning electron micrographs and the corresponding chemical microanalysis performed by energy dissipative x-ray spectroscopy (EDS) of the surface of the modified glassy carbon electrode after each step of the grafting procedure of Fig. 1.

The surface of the bare GC working electrode is quite smooth (Fig. 3a); the corresponding carbon and oxygen EDS peaks indicate that the surface contamination is quite low. The surface morphology of the electrode after diazonium derivative grafting and after Co-clathrochelate functionalization are shown on Fig. 3b and c, respectively. The roughness of the surface is significantly increased, as a result of the grafting of the diazonium derivative. The surface morphology of the electrode after the diazonium electrografting step and after the chemical grafting of the cobalt clathrochelate step was found mostly unchanged (Fig. 3b and c). Our initial objective was to use electro-grafting to obtain surface molecular monolayers. The GC electrode surface was polished but in spite of this remains quite rough. In addition, this is not a perfectly ordered surface (the microstructure is not constant at the local scale). This is why we assume that the surface mat might contain several layers, stacked to each other, as observed by atomic force microscopy (Fig. 4). Moreover, the EDS spectrum indicates an increase of nitrogen atoms as well as the appearance of a peak related to the

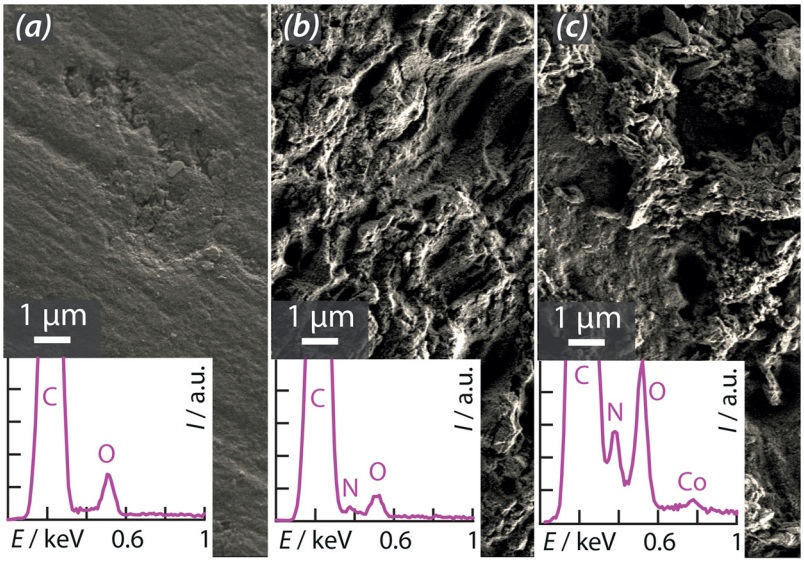

Fig. 3. Scanning electron micrographs and corresponding EDS spectra of (a) the bare glassy carbon electrode, (b) the catalytic modified electrode after diazonium derivative grafting, (c) the catalytic modified electrode after Co clathrochelate grafting.

presence of Co atoms that confirms the grafting of the Co clathrochelate onto the carbon electrode.

3.5. Atomic force microscopy

PeakForce tapping atomic force microscopy analysis was performed on the bare glassy carbon and the modified electrode after electrografting of the clathrochelate electrocatalyst. The resulting topology and peakforce error images are displayed on Fig. 4. The image showing surface topology unambiguously indicates that the surface of the bare GC working electrode (lower part of the image on Fig. 4a) is smooth whereas the electrocatalyst deposit is clearly observed on the modified area of the sample (upper part of the AFM image on Fig. 4a). The catalyst layer was found to be approximately 15 nm thick and homogeneously deposited over the entire substrate surface. The information obtained by AFM analysis is consistent with the observation obtained by SEM. Our initial objective was to use electro-grafting to obtain surface molecular monolayers. However, the 15-nm thick electrocatalytic layer (diazonium derivative/Co clathrochelate) observed by AFM indicates that a multi layer films was obtained instead. A smoother carbon surface, such as graphene, could perhaps circumvent this problem and lead to real monolayers. However, this was not investigated. Some side-reactions occurring during the different steps of the electrografting reaction and leading to the formation of insoluble residues at the surface could also take place.

The peakforce error signal (Fig. 4b) displays two different areas showing the force interaction of the AFM probe with the surface. The force appeared to be stronger when interacting with the functionalized area of the electrode.

3.6. X-ray photoelectron spectroscopy

The solid glassy carbon working electrode surface covered with the diazonium derivative and the Co clathrochelate complex was further characterized by XPS spectroscopy. The core level spectra of N1s and Co2p [energy levels] are shown on Fig. 5, after each step of the Co clathrochelate grafting processes (see Fig. 1). The N1s core level peak could be decomposed as the sum of different contributions. The 400 eV component was consistent with the presence of amino groups and N—C bonds at the electrode surface whereas a component at 406 eV was related to NO_2 groups. A third component at 402 eV was likely correspond to N—O and NH—C═O bonds. The presence of a small component at lower energy (398 eV) was attributed to the partial reduction of some grafted nitrophenyl diazonium functions on the surface, corresponding to negatively charged N atoms at the surface of the electrode [37]. Fig. 5b shows the decrease of the peak at 406 eV and the increase of the peak at 400 eV. This confirms the almost complete reduction of nitrophenyl functions to aminophenyl over the surface of the electrode

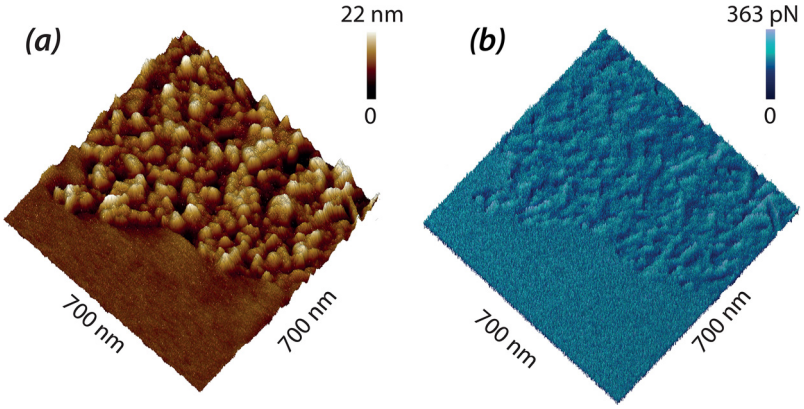

Fig. 4. (a) Atomic force microscope images displaying the topology of the bare GC electrode surface (lower part) and the modified electrode surface by the Co-electrografted catalyst (upper part) and (b) the corresponding error-force image.

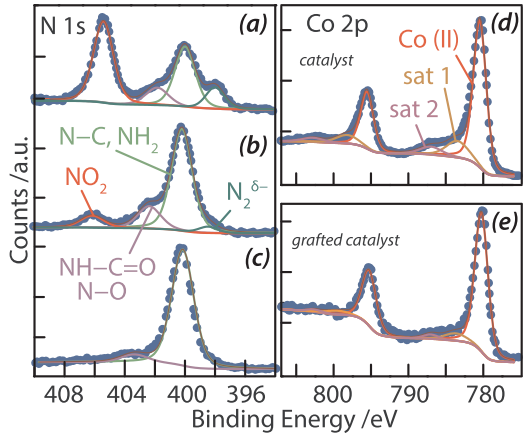

Fig. 5. X-ray photoelectron spectroscopy spectra corresponding to N1s energy level of (a) the modified solid-electrode after diazonium derivative grafting, (b) the modified solid-electrode after electroreduction of diazonium derivative to Ph-NO_2, (c) the modified solid-electrode after Co clathrochelate grafting and Co2p energy level of (d) Co clathrochelate catalyst and (e) electrografted Co clathrochelate to modified solid-electrode.

[38,39]. The smaller components at 398 eV, often observed experimentally but still prone to debate, may be attributed to the formation of azo bridges in the film. It is well-established that diazonium is prone to coupling, resulting in the formation of an azobenzene derivative forming during the film growth [40]. Furthermore, such azo bridges could be formed at the surface and within the film. The peak at 398 eV disappeared after reduction of the diazonium salt: this indicates the total disappearance of residual diazonium derivatives.

Fig. 5c shows the decrease of the NH–C = O peak as well as the total disappearance of the NO_2 peak which confirms the covalent grafting of the catalytic complex over the surface of the glassy carbon working electrode. Furthermore, the presence of cobalt at the surface of the electrode confirms the success of electro-grafting (Fig. 5d). A comparison of the XPS spectra of the cobalt clathrochelate in the powder form (Fig. 5e) and after electrografting over the glassy carbon electrode (Fig. 5d) leads to the conclusion that the chemical environment of the Co metal center was not modified during grafting. The oxidation state of the Co active centre is + II in the powder and remains unchanged after electrografting [41].

3.7. Electrochemistry of the cobalt clathrochelate in solution

The electrochemical behavior of the cobalt clathrochelate in solution (in acetonitrile) was analyzed by cyclic voltammetry. Results are plotted in Fig. 6.

The different CVs of Fig. 6a show two characteristic electrochemical waves, corresponding to the two monoelectronic redox reactions of the cobalt complex: Co^{III}/Co^{II} at –0.1 V and Co^{II}/Co^{I} at –1.2 V (potentials are referred vs. Fc^+/Fc). The potential difference at peak currents was found to increase with the potential scan rate, for both redox couples. The linear dependence of peak currents density with the square root of the scan rate (Fig. 6b and c) indicates that the electron transfer process is mainly diffusion-controlled. The electroactivity of the cobalt clathrochelate dissolved in solution in acetonitrile with regard to the HER was put into evidence by cyclic voltammetry, by adding increasing amounts of protons to the solution. An aqueous solution of formic acid (equivalent of 4 mM) was used as H^+ source. The resulting CVs are plotted on Fig. 7. Upon proton addition, the onset of the HER is at approximately –1.5 V. Current density values are proportional to the proton concentration (measures have been made from 0 to 20 proton equivalents). Such behavior is characteristic of a catalytic effect. A maximum current density value of –0.25 mA cm^{-2} was measured at –2.4 V for 20 proton equivalents. It has to be noted that no catalytic effect was observed in the absence of cobalt clathrochelate (see CVs in Supplementary, Fig. S1).

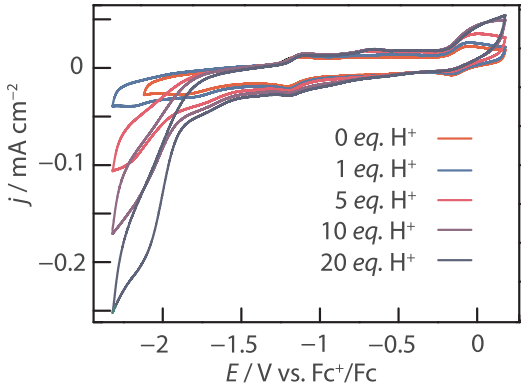

Fig. 7. Electrocatalytic hydrogen evolution reaction of Co clathrochelate in the solution (acetonitrile + TBAP 0.1 M) with addition of equivalents of HCOOH as H^+ source. Scanning rate: ν = 30 mV s^{-1}.

It has to be noted that some geometrical parameters can be taken into consideration in order to evaluate the impact of the different substituents of the cage framework surrounding the cobalt center of the clathrochelate molecule on the electrochemical properties of the catalytic complex as we suggested in previous paper [41]. Density functional theory calculations have been performed in order to determine the bond length and bond angle of the Co–N (Supplementary, Fig. S2).

3.8. Electrochemistry of the electrografted cobalt clathrochelate

Fig. 8 shows the CVs recorded on the Co-grafted glassy carbon working electrode. Measurements have been made at different scan rates, in a solution of dimethylformamide, using TPAB as supporting electrolyte. The redox features observed with the complex in solution are less pronounced but still identifiable. This is attributed to the fact that the surface amounts of complex are significantly less than what was used in solution. The peak potential separation of the anodic and cathodic waves ($\Delta E_p = E_{pa} - E_{pc}$) was found to increase with the scan

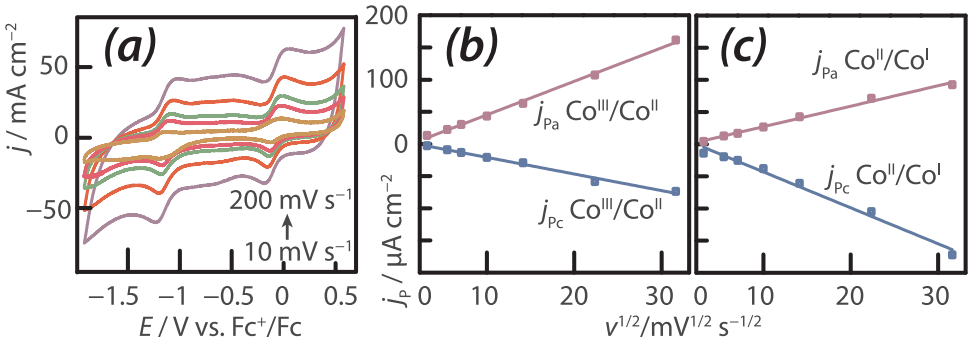

Fig. 6. (a) Cyclic voltammograms of the Co-catalyst in the homogeneous phase at different scan rates (10, 30, 50, 100, 200 mV s^{-1}) in acetonitrile + 0.1 M TBAP as supporting electrolyte. (b,c) Evolution of anodic and cathodic current density peaks corresponding to peak potentials of the two redox couples Co^{III}/Co^{II} and Co^{II}/Co^{I} of the Co clathrochelate.

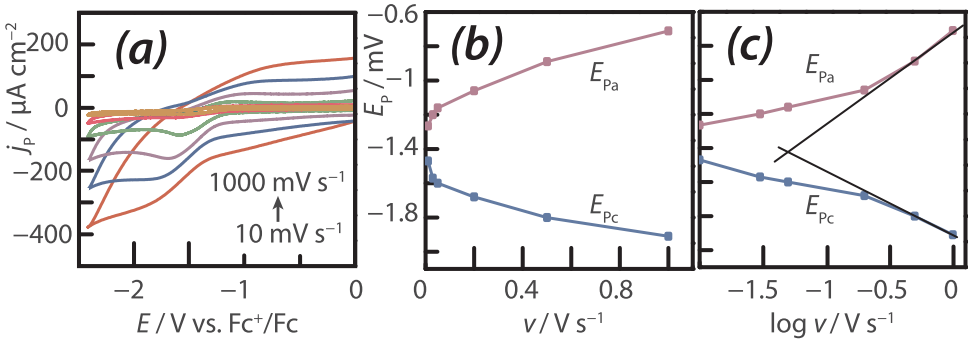

Fig. 8. (a) Cyclic voltammograms of the catalytic modified electrode by the grafted catalyst at different scan rates (10, 30, 50, 100, 200, 500, 1000 mV s^{-1}) in dimethylformamide + 0.1 M TBAP. Evolution of anodic and cathodic potential peaks as a function of the scanning rate (b) and as a function of the log of scanning rate (c).

Table 1
Anodic and cathodic potentials of the Co^{II}/Co^{I} electrochemical wave and corresponding peak separation $|\Delta E_p|$ of the clathrochelate grafted to the solid carbon electrode.

Scanning rate (mV s^{-1})	E_{pa} Co^{II}/Co^{I} (mV)	E_{pc} Co^{II}/Co^{I} (mV)	$\|\Delta E_p\|$ (mV)	$E°$ (mV)
1000	−710	−1910	1200	−1310
500	−890	−1800	910	−1345
200	−1060	−1680	620	−1370
50	−1160	−1600	440	−1380
30	−1200	−1570	370	−1385
10	−1266	−1470	205	−1368

rate (Fig. 8a and b).

Quantitative values are compiled in Table 1. Additional UV–vis spectrometry measurements were performed in order to assess the chemical stability of the clathrochelate in acidic medium during the experiments (Supplementary, Fig. S3). Additional electrochemical information was extracted from these data using the so-called Laviron method [42]. For monoelectronic (n = 1) electrochemical charge transfer reactions, when experimental $\Delta E_p/n$ values are larger than 200 mV (this is the case here), the charge transfer coefficient (α) and the rate constant of the electrochemical reaction [k^0 (in s^{-1})] can be determined by using the following set of equations [42]:

$$E_{pa} = E° + \frac{RT}{(1-\alpha)nF}\ln\frac{(1-\alpha)}{m} \quad (1)$$

and

$$E_{pc} = E° - \frac{RT}{\alpha nF}\ln\frac{\alpha}{|m|} \quad (2)$$

where

$$m = \frac{RT}{F}\frac{k^0}{nv}$$

R is the ideal gas constant, T the absolute temperature and v the potential scan rate. Plots of $E_{pa} = f(\log v)$ and $E_{pc} = f(\log v)$ yield two straight lines (Fig. 8c). Their slopes are equal to –2.3 $RT/\alpha nF$ for the cathodic peak, and 2.3 $RT/(1–\alpha)nF$ for the anodic peak. The α values can be determined from the experimental slopes. The slope of the straight line corresponding to the cathodic reaction was determined to be equal to 400 mV/log unit. The resulting α coefficients of the cathodic and anodic reactions were found to be equal to 0.15 and 0.85 respectively.

According to the same method [42], the k^0 values can be calculated using the following Eq. (3):

$$\log k^0 = \alpha\log(1-\alpha) + (1-\alpha)\log\alpha - \log\frac{RT}{nFv} - \alpha(1-\alpha)\frac{nF\eta}{2.3RT} \quad (3)$$

After rearrangement of Eq. (3) for $\eta = E - E° = 0$, one obtains:

$$k^0 = \frac{\alpha nFv_c}{RT} = (1-\alpha)\frac{\alpha nFv_a}{RT} \quad (4)$$

The anodic and cathodic k^0 values determined for $v_a = v_c = 1$ V s^{-1} are $k^0 = 3.89$ s^{-1} and $k^0 = 33$ s^{-1}, respectively.

The variations of peak current potentials as a function of the potential scan rates are plotted in Fig. 8b. According to Ref. [42], such behavior could be attributed to a series of molecules having a N=N double bond, such as phenazine, azobenzene, an explanation consistent with the fact that the clathrochelate used here (see Fig. 1) has multiple N=N bonds and for which both the oxidized and the reduced forms are strongly adsorbed. The shape of the experimental isotherm is that of a Langmuir isotherm, valid for low surface coverages, as suggested in [37].

The complex-modified GC working electrode was further characterized by addition of increasing amounts of protons to the solution, in order to evaluate its HER activity. Fig. 9a shows the CVs obtained by adding increasing amounts of an aqueous solution of formic acid (up to 4 mM) to the electrochemical cell. On the cathodic side, current plateaus related to diffusion-controlled proton transfers to the interface are observed. Current plateau values increase with proton concentration, unequivocally showing the electrocatalytic effect of the cobalt complex on the HER. Compared to the situation in the homogeneous phase, a large overpotential decrease (of approximately 800 mV vs. Fc^+/Fc) is obtained after surface electrografting (see Fig. 9b): the onset of the HER on the modified GC working electrode starts at more positive potentials values. Electrochemical impedance spectroscopy was also used to provide an insight on the electrochemical process taking place in the current plateau region. In the high frequency region (Fig. 9c), EIS impedance diagrams show a single depressed semicircle corresponding to a slow charge transfer step (at about 1 Hz). In the low frequency domain (for frequencies lower than 40 mHz), a 45° semi-infinite semi-line characteristic of a diffusion-controlled step consistent with the data of

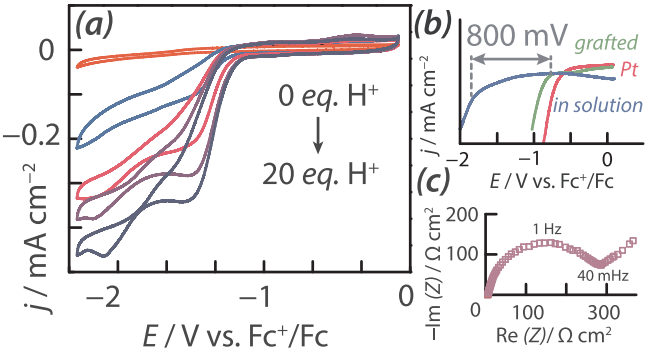

Fig. 9. (a) Cyclic voltammograms recorded on the GC electrode with electrografted Co-clathrochelate in dimethylformamide + 0.1 M TBAP with increasing amounts of H^+ (HCOOH is the H^+ source). (b) Overpotential differences between the 3 systems under consideration (20 H^+ equivalents). (c) EIS spectrum in Nyquist coordinates measured on the GC electrode with electrografted Co-clathrochelate (E = −2 V vs. Fc^+/Fc). Scanning rate: v = 30 mV s^{-1}.

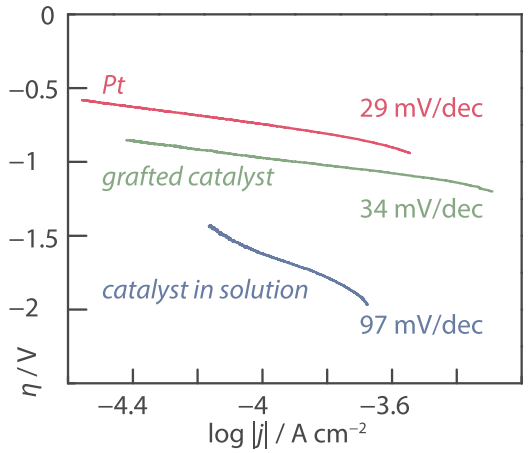

Fig. 10. Tafel plots recorded on a GC working electrode (i) in contact with a 0.2 mM Co-clathrochelate solution; (ii) electro-grafted with the Co-clathrochelate catalyst and (iii) on Pt (reference case) in acetonitrile + 0.1 M TBAP + 4 mM of HCOOH as H^+ source.

Fig. 9a is also observed. This limitation can be attributed to the low proton concentration in this non aqueous electrolyte and/or possibly to the porous structure of the Co clathrochelate layer formed over the glassy carbon surface. Both factors can possibly contribute to proton diffusion.

Experimental Tafel plots were fitted to the conventional Tafel equation ($\eta = b \log j + a$, where j is the current density and b is the Tafel slope). Data are plotted on Fig. 10. For the HER, a Tafel slope of 30 mV/decade corresponds to a fast surface discharge followed by a rate-determining chemical desorption [43]. This is what is obtained here for Pt and for the electrografted GC electrode. The larger slope measured when the complex is dissolved in solution might be more consistent with a diffusion-controlled mechanism or a mix transport-transfer mechanism. The low exchange current density values (Table 2) are explained by the low proton concentration in solution.

The stationary hydrogen production rate in both homogeneous and heterogeneous conditions was determined by gas chromatography titration during chronopotentiometric experiments. A three-compartment cell (cathode, anode and reference electrode) was used to maintain a high (close to unity) faradaic efficiency. Results are shown in Fig. 11. These measurements confirm the higher hydrogen production rate obtained once the cobalt complex is grafted onto the GC working electrode. A two times lower H_2 production rate was measured in the homogeneous phase compared to the electrografted GC working electrode (4.85 $\mu mol_{H2}\, h^{-1}\, cm^{-2}$) against 9.55 $\mu mol_{H2}\, h^{-1}\, cm^{-2}$). The Co complexes are involved in the HER mechanism. When the Co complexes are dissolved in solution, their diffusion-controlled transport to/from the interface make the overall kinetics lower than when the Co complexes are electrografted at the surface of the electrode. This is a situation closer to what is observed on Pt.

In conclusion, it can be said that the GC working electrode with electrografted Co-clathrochelate is not as good as Pt but better than bare GC with the complex in solution. The complex is a good candidate for the HER in acidic media and comparable to other systems of the literature [44].

Finally, in order to get closer to operating conditions of practical interest, measurements have been made directly in aqueous acidic conditions (0.1 M H_2SO_4, pH ≈ 1). The cobalt complex was found sufficiently stable over hours to perform the experiments. Fig. 12a shows the linear sweep voltammograms measured on bare glassy carbon, with the clathrochelate electrografted at the surface, and again on platinum for comparison. For comparison, the clathrochelate binded to the surface with a sulfonated tetrafluoroethylene based fluoropolymer-copolymer, the so-called Nafion®, (see Supplementary, Fig. S4) was also characterized in acidic medium. It was observed that the HER started at a higher overpotential than that compared with electrografted Co-clathrochelate at GC electrode. Note that this experiment cannot be performed in acetonitrile with the addition of controlled amounts of proton since recast Nafion® films are not stable in this medium, leading to the piling off of the catalytic film. Fig. 12b shows the corresponding Tafel slopes. For Pt, the situation remains unchanged but for the GC electrode in contact with the Co-complex, significantly larger slopes are measured. Slopes close to 120 mV/decade are usually ascribed to a rate-determining discharge step. Larger values such as those measured here on bare GC and with the Co-complex electrografted may indicate the onset of other reaction paths (e.g. mass transport contributions or reaction steps involving chemical interactions with the Co-complex) that will require further characterization. Exchange current density values are compiled in Table 2, and compared to those measured in acetonitrile + 4 mM HCOOH. In 0.1 M H_2SO_4, the gain in HER overvoltage after electrografting is significantly less pronounced but still, the electrografted provides high HER electroactivity (see also Supplementary, Fig. S5). All these results provide a proof-of-concept for the use of this cobalt clathrochelate electrografted on glassy carbon in water electrolysis. Our results are put in a broader perspective in the Table S6, which presents the performance of our Co clathrochelate grafted to the GC electrode in terms of overpotential for HER featuring some Co-based electrocatalysts functionalized on modified electrodes and massive Co-based electrodes in aqueous acidic conditions. We observe that our Co clathrochelate modified planar electrode exhibits a higher overpotential than 3D electrodes modified by Co complexes. Moreover, it loses its competitiveness when compared to massive cobalt-based systems such as thin film layers.

4. Conclusions

In an attempt to find alternative electrocatalysts to platinum group metals, we report on the electrochemical activity of a cobalt clathrochelate electrocatalyst with regard to the HER. In such complex, the catalytically active Co center is embedded in a macrobicyclic tris-dioximate ligand cage. Measurements have been made using glassy carbon as working electrode in two complementary configurations: in the homogeneous phase (the active complex is dissolved in the electrolyte) and in the heterogeneous phase (the complex is electrografted at the surface of the GC working electrode). The surface functionalization of the Co-complex was achieved by electrografting via the electrochemical reduction of in situ generated aminophenyl diazonium. Experimental results measured in acetonitrile in the presence of controlled amounts of protons show that the glassy carbon working electrode is more active when the cobalt clathrochelate is electrografted instead of being dissolved in solution. A reduction of approximately 800 mV of the HER overvoltage was measured, leading to much higher current density values. The GC modified electrode has also been tested in aqueous 0.1 M H_2SO_4 solution (pH = 1) in view of practical applications in water electrolysers. Despite the low electrolyte pH, the

Table 2
Log of HER exchange current densities ($\log|j_0|$, j_0 in A. cm^{-2}) of the two electrodes in the two different media.

$\log\|j_0\|$ (j_0 in A. cm^{-2})	Bare GC	Co-complex in solution	Co-complex electro-grafted@GC	Pt
acetonitrile + 4 mM HCOOH	–	−6	−5.5	−5.2
0.1 M H_2SO_4	−5	–	−4.6	−2.8

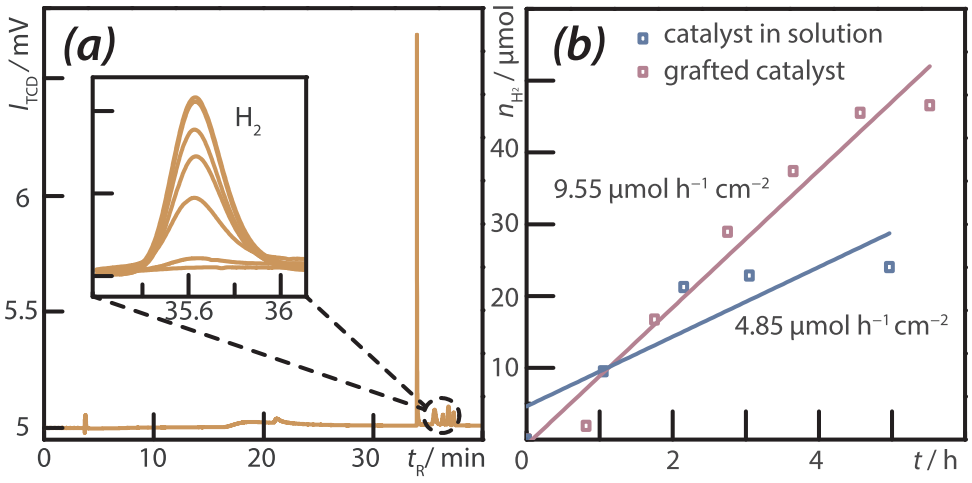

Fig. 11. (a) Typical gas chromatography spectrum showing H_2 produced during electrolysis in acetonitrile + 0.1 M TBAP + 20 H^+ eq (using HCOOH). (b) Quantitative comparison of H_2 production rates using the catalyst in solution and the electrografted catalyst (1 cm^2 surface area; E = – 1.9 V vs. Fc^+/Fc).

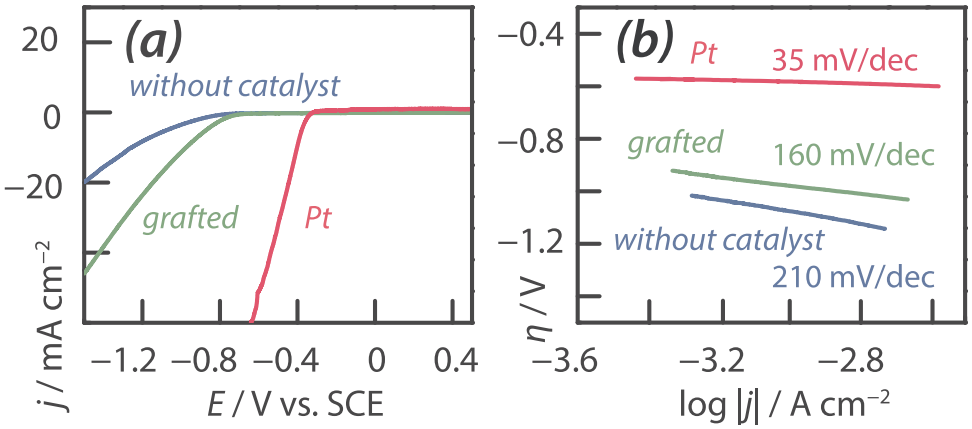

Fig. 12. (a) Cyclic voltammograms and (b) Tafel plots recorded on bare GC electrode (without catalyst), on the electrografted Co clathrochelate@GC electrode, and on Pt as a reference, respectively. The electrolyte contained 0.1 M H_2SO_4 in water.
Scanning rate: ν = 30 mV s^{-1}.

chemical stability of the electro-grafted complex was found sufficient to perform the experiments.

Acknowledgments

The authors gratefully acknowledge Dr. François Brisset for technical support with SEM characterization. Joumada Al Cheikh was indebted to a PhD scholarship of Azm & Saade Association (Lebanon). Momentom IRS project from IDEX Université Paris-Saclay is acknowledged for funding. This work was supported by a public grant provided by the French National Research Agency (ANR) as part of the "Investissements d'Avenir" program (Labex Charmmmat, ANR-11-LABX-0039-grant).

Appendix A. Supplementary data

Supplementary material related to this article can be found, in the online version, at doi:https://doi.org/10.1016/j.apcatb.2019.03.036.

References

[1] P. Millet, A. Godula-Jopek, D. Stolen (Eds.), Hydrogen Production by Electrolysis, Wiley-VCH, 2015, pp. 1–395.
[2] D. Bessarabov, P. Millet, B.G. Pollet (Ed.), PEM Water Electrolysis, Elsevier, 2018, pp. 1–176.
[3] H.A. Gasteiger, S.S. Kocha, B. Sompalli, F.T. Wagner, Activity benchmarks and requirements for Pt, Pt-alloy, and non-Pt oxygen reduction catalysts for PEMFCs, App. Catal. B: Environ. 56 (2006) 9–35.
[4] Z. Guo, X. Wang, Atomic layer deposition of the metal pyrites FeS_2, CoS_2, and NiS_2, Angew. Chem. Int. Ed. 57 (2018) 5898–5902.
[5] D. Khusnutdinova, B.L. Wadsworth, M. Flores, A.M. Beiler, E.A.R. Cruz, Y. Zenkov, G.F. Moore, Electrocatalytic properties of binuclear Cu(II) fused porphyrins for hydrogen evolution, ACS Catal. 8 (2018) 9888–9898.
[6] Z. Wei, Y. Yang, M. Liu, J. Dong, X. Fan, X.M. Zhang, Cobalt nanocrystals embedded into N-doped carbon as highly active bifunctional electrocatalysts from pyrolysis of triazolebenzoate complex, Electrochem. Acta 284 (2018) 733–741.
[7] I.K. Mishra, H. Zhou, J. Sun, F. Qin, K. Dahal, J. Bao, S. Chen, Z.F. Ren, Hierarchical CoP/Ni_5P_4/CoP microsheet arrays as a robust pH-universal electrocatalyst for efficient hydrogen generation, Energy Environ. Sci. 11 (2018) 2246–2252.
[8] P. Millet, Conventional and innovative electrocatalysts for PEM water electrolysis, ECS Trans. 75 (14) (2016) 28–35.
[9] T. Abe, M. Kaneko, pH-dependent electrocatalysis for proton reduction by bis (2,2′:6′,2″-terpyridine) cobalt(II) complex embedded in nafion® membrane, J. Mol. Catal. A: Chem. 169 (2001) 177–183.
[10] B.J. Fisher, R. Eisenberg, Electrocatalytic reduction of carbon dioxide by using macrocycles of nickel and cobalt, J. Am. Chem. Soc. 102 (1980) 7361–7363.
[11] C.V. Krishnan, N. Sutin, Homogeneous catalysis of the photoreduction of water by visible light. 2. Mediation by a tris(2,2′-bipyridine)ruthenium(II)-cobalt(II) bipyridine system, J. Am. Chem. Soc. 103 (1981) 2141–2142.
[12] V. Houlding, T. Geiger, U. Kölle, M. Grätzel, Electrochemical and photochemical investigations of two novel Electron relays for hydrogen generation from water, J. Chem. Soc. Chem. Commun. 12 (1982) 681–683.
[13] J.M. Lehn, R. Ziessel, Photochemical generation of carbon monoxide and hydrogen by reduction of carbon dioxide and water under visible light irradiation proc, Natl. Acad. Sci. 79 (1982) 701–704.
[14] R.M. Kellett, T.G. Spiro, Cobalt(I) porphyrin catalysts of hydrogen production from water, Inorg. Chem. 24 (1985) 2373–2377.
[15] U. Kölle, S. Ohst, Electrochemical reduction of protonated cyclopentadienylcobalt phosphine complexes, Inorg. Chem. 25 (1986) 2689–2694.

[16] S. Schlicht, L. Assaud, M. Hansen, M. Lickleder, M. Bechelany, M. Perner, J. Bachmann, An electrochemically functional layer of Hydrogenase extract on an electrode of large and tunable specific surface area, J. Mater. Chem. A 4 (2016) 6487–6494.
[17] J. Lyskawa, D. Bélanger, Direct modification of a gold electrode with aminophenyl groups by electrochemical reduction of in situ generated aminophenyl monodiazonium cations, Chem. Mater. 18 (2006) 4755–4763.
[18] L. Assaud, N. Massonnet, D. Evrard, H. Vergnes, L. Salvagnac, V. Conédéra, L. Noé, M. Monthioux, P. Gros, P. Temple-Boyer, B. Caussat, A new route for the integration of a graphene/diazonium/PEDOT electrode towards antioxidant biomarker detection, J. Electroanal. Chem. 771 (2016) 73–79.
[19] D. Bélanger, Pinson, Electrografting: a powerful method for surface modification, J. Chem. Soc. Rev. 40 (2011) 3995–4048.
[20] O. Pantani, S. Kaskar, R. Guillot, P. Millet, E. Anxolabéhère, A. Aukauloo, Cobalt clathrochelate complexes as hydrogen-producing catalysts, Angew. Chem. Int. Ed. 120 (2008) 10096–10098.
[21] M.L. Rigsby, S. Mandal, W. Nam, L.C. Spencer, A. Llobet, S.S. Stahl, Cobalt analogs of Ru-based water oxidation catalysts: overcoming thermodynamic istability and kinetic lability to achieve electrocatalytic O_2, Evol. Chem. Sci. 3 (2012) 3058–3062.
[22] C.F. Leung, S.M. Ng, C.C. Ko, W.L. Man, J. Wu, L. Chen, T.C. Lau, A cobalt(II) quaterpyridine complex as a visible light-driven catalyst for both water oxidation and reduction, Energy Environ. Sci. 5 (2012) 7903–7907.
[23] D. Wang, J.T. Groves, Efficient water oxidation catalyzed by homogeneous cationic cobalt porphyrins with critical roles for the buffer base, Proc. Natl. Acad. Sci. 110 (2013) 15579–15584.
[24] T. Nakazono, A.R. Parent, K. Sakai, Cobalt porphyrins as homogeneous catalysts for water oxidation, Chem. Commun. 49 (2013) 6325–6327.
[25] N. Kaeffer, M. Chavarot-Kerlidou, V. Artero, Hydrogen evolution catalyzed by cobalt diimine–dioxime complexes, Acc. Chem. Res. 48 (2015) 1286–1295.
[26] X. Hu, B.S. Brunschwig, J.C. Peters, Electrocatalytic hydrogen evolution at low overpotentials by cobalt macrocyclic glyoxime and tetraimine complexes, J. Am. Chem. Soc. 129 (2007) 8988–8998.
[27] Y.Z. Voloshin, O.A. Varzatskii, I.I. Vorontsov, M. Yu Antipin, Tuning a metal's oxidation state: the potential of clathrochelate systems, Angew. Chem. Int. Ed. 44 (2005) 3400–3402.
[28] B.S. Furniss, A.J. Hannaford, P.W.G. Smith, A.R. Tatchell, Volgel's Textbook of Pratical Organic Chemistry, 5th edn, Longman, London, 1989, p. 920.
[29] S. Baranton, D. Bélanger, Electrochemical derivatization of carbon surface by reduction of in situ generated diazonium cations, J. Phys. Chem. B 109 (2005) 24401–24410.
[30] K.K. Cline, L. Baxter, D. Lockwood, R. Saylor, A. Stalzer, Nonaqueous synthesis and reduction of diazonium ions (without isolation) to modify glassy carbon electrodes using mild electrografting conditions, J. Electroanal. Chem. 633 (2009) 283–290.
[31] F. Barrière, A.J. Downard, Covalent modification of graphitic carbon substrates by non-electrochemical methods, J. Solid State Electrochem. 12 (2008) 1231–1244.
[32] T. Suehiro, S. Masuda, T. Tashiro, R. Nakausa, M. Taguchi, A. Koike, A. Rieker, Formation and identification of aryldiazenyl radicals using the ESR technique bull, Chem. Soc. Jpn. 59 (1986) 1877.
[33] T. Suehiro, S. Masuda, R. Nakausa, M. Taguchi, M. Mori, A. Koike, M. Date, Moiré Pattern of bilayered fatty acid monolayers based on dark field imaging, Bull. Chem. Soc. Jpn. 120 (1998) 3247.
[34] J.M. Savéant, Electron transfer, bond breaking and bond formation, Adv. Phys. Org. Chem. 35 (2000) 117–192.
[35] C.P. Andrieux, J. Pinson, The standard redox potential of the phenyl radical/anion couple, J. Am. Chem. Soc. 125 (2003) 14801–14806.
[36] M. Delamar, R. Hitmi, J. Pinson, J.M. Savéant, Covalent modification of carbon surfaces by grafting of functionalized aryl radicals produced from electrochemical reduction of diazonium salts, J. Am. Chem. Soc. 114 (1992) 5883–5884.
[37] P. Chambrion, T. Suzuki, Z.G. Zhang, T. Kyotani, A. Tomita, XPS of nitrogen-containing functional groups formed during the C−NO reaction, Energy Fuels 11 (1997) 681–685.
[38] N. Graf, E. Yegen, T. Gross, A. Lippitz, W. Weigel, S. Krakert, A. Terfort, W.E.S. Unger, XPS and NEXAFS studies of aliphatic and aromatic amine species on functionalized surfaces, Surf. Sci. 603 (2009) 2849–2860.
[39] P. Allongue, M. Delamar, B. Desbat, O. Fagebaume, R. Hitmi, J. Pinson, J.M. Savéant, Covalent modification of carbon surfaces by aryl radicals generated from the electrochemical reduction of diazonium salts, J. Am. Chem. Soc. 119 (1997) 201–207.
[40] B. Hurley, R.L. McCreery, Covalent bonding of organic molecules to Cu and Al alloy 2024 T3 surfaces via diazonium ion reduction, J. Electrochem. Soc. 151 (2004) B252–B259.
[41] M. Antuch, A. Ranjbari, S.A. Grigoriev, J. Al-Cheikh, A. Villagrá, L. Assaud, Y.Z. Voloshin, P. Millet, Effect of the ligand framework of cobalt clathrochelates on hydrogen evolution electrocatalysis: electrochemical, spectroscopic and density functional theory analyses, Electrochim. Acta 245 (2017) 1065–1074.
[42] E. Laviron, General expression of the linear potential sweep voltammogram in the case of diffusionless electrochemical systems, J. Electroanal. Chem. Inter. Electrochem. 101 (1979) 19–28.
[43] L. Liao, J. Zhu, X. Bian, L. Zhu, M.D. Scanlon, H.H. Girault, B. Liu, MoS_2 formed on mesoporous graphene as a highly active catalyst for hydrogen evolution, Adv. Funct. Mater. 23 (2013) 5326–5333.
[44] N. Coutard, N. Kaeffer, V. Artero, Molecular engineered nanomaterials for catalytic hydrogen evolution and oxidation, Chem. Commun. 52 (2016) 13728–13748.